Research Article Vol. 31, No. 26 / 18 Dec 2023 / Optics Express 43427
Optics EXPRESS

Gain-managed nonlinear amplification of ultra-long mode-locked fiber laser

D. STOLIAROV,* E. MANUYLOVICH, A. KOVIAROV, D. GALIAKHMETOVA, AND E. RAFAILOV

Aston Institute of Photonic Technologies, College of Engineering and Physical Sciences, Aston University B4 7ET Birmingham, United Kingdom
*d.stoliarov@aston.ac.uk

Abstract: In this study, we explored the gain-managed nonlinear (GMN) amplification of ultra-low repetition rate pulses in the range of less than 1 MHz. By seeding the developed 1040 nm ultralong fiber modelocked laser to the GMN amplifier, we achieved high gain and boosted the nonlinear pulse propagation effects. We demonstrated that GMN amplification of low repetition rate pulses provided amplification exceeding 32 dB and spectral broadening up to 91 nm at relatively low pump power levels. Achieving broadband 57 fs pulses with energy exceeding 55 nJ suggests that ultralong fiber lasers paired with GMN amplifiers can be effectively utilized as powerful tools for generating femtosecond broadband pulses at ultra-low repetition rates, with controllable spectral characteristics.

1. Introduction

Over the past decades, there has been an increased interest in high-power ultrafast fiber lasers and master-oscillator power-amplifier (MOPA) systems, which are attractive for a broad range of applications, from medicine to micro-machining, driving continued research into developing innovative source configurations with improved pulse characteristics and reliability [1,2]. Fiber amplifiers play a critical role in MOPA systems as they can significantly affect the seed pulse properties during amplification. Gain narrowing and nonlinear effects pose challenges to pulse quality.

High-peak-intensity ultrafast fiber lasers offer numerous advantages over their solid-state counterparts, such as compactness, excellent thermo-optical properties, and superior beam quality. However, the confinement of high-peak-power pulses in a small core over long propagation distances leads to the accumulation of significant nonlinear effects that can degrade pulse quality. Chirped-pulse amplification (CPA) [3] is commonly used for high-energy sources but has limitations such as gain narrowing and residual dispersion mismatch [2,4]. Consequently, alternative techniques leveraging nonlinear pulse propagation, such as direct amplification [5], including pre-chirp management [6–9], including the parabolic pre-shaping [10] and self-similar pulse evolution [11,12], have been developed to achieve sub-100-fs pulse durations.

Recently GMN amplification has been proposed as a new nonlinear amplification scheme [13]. Unlike Mamyshev oscillators that use the self-phase modulation and offset filtering for stable, periodic pulse evolution via nonlinear propagation in the laser cavity, the unidirectional, single-pass GMN technique focuses on controlling nonlinear effects during amplification to optimize pulse parameters [14]. In GMN amplifiers, a narrowband seed pulse experiences significant spectral broadening but is still compressible to a near-transform-limited duration using a standard grating compressor. The GMN amplification regime is driven by a nonlinear attractor, making it relatively insensitive to the seed pulse and more accessible for a wider range of input pulses [13]. The combination of the Mamyshev oscillator and gain-managed amplifier

#510017 https://doi.org/10.1364/OE.510017
Journal © 2023 Received 20 Oct 2023; revised 28 Nov 2023; accepted 28 Nov 2023; published 7 Dec 2023

Optics EXPRESS

for achieving high-power ultrashort pulse durations has recently been introduced within an all-PM-fiber linear laser scheme featuring a pump-modulated oscillator. This approach allows for pulse energies exceeding 100 nJ [15].

GMN amplifiers have been experimentally demonstrated in large mode area (LMA) 30/125 gain fibers, achieving pulse energies up to 1.2 μJ with a pulse repetition rate (PRR) of 5.4 MHz [16]. This approach enables the pulse energy scaling with mode area while maintaining pulse quality, as the intricate balance of nonlinear spectral broadening and gain shaping is preserved. The GMN regime has been successfully extended to LMA fibers with 30 μm core, providing a promising solution for the generation of high-power broadband ultrashort pulses. In a comparative study of GMN amplifiers, two lasers with pulse durations of 226 fs and 268 fs and different repetition rates of 125 MHz and 30 MHz, respectively, were used as seed sources [17]. This study demonstrated the differences in spectral broadening beyond the conventional doped fiber gain window [9,18]. For conventional Yb-doped fiber, it is effectively limited by 1100 nm. The obtained spectra for the lower-repetition-rate source were slightly broader and therefore supported shorter pulse durations but were limited by 1150 nm by occurring interference between secondary pulse structures separated in time around this wavelength region that appears due to Raman scattering.

All previous studies of GMN amplification were focused on the evolution of femtosecond pulses with a common pulse repetition rate (PRR) typical of mode-locked fiber lasers, ranging from 10-125 MHz. However, many applications necessitate a lower PRR (less than 1 MHz) for ultrashort pulses [19,20]. The ultra-low repetition rate diminishes the laser's average power, which minimizes heat accumulation in the target material. This is of paramount importance in material processing and medical fields to avert undesired thermal damages [21,22]. Additionally, high-power, low-PRR lasers can invoke nonlinear effects in the target material, paving the way for applications such as multiphoton microscopy or frequency conversion. Such effects can be instrumental, unveiling novel imaging and diagnostic methods in the medical sector [23]. In our research, we underline our accomplishment in achieving high pulse energy and short pulse duration in the low rep rate domain. This is particularly pivotal for scenarios where a low average power is imperative, but there's a demand for high peak power and pulse energy.

While ultrashort pulses with low repetition rates are advantageous in enhancing precision, mitigating collateral damage, and ensuring superior control in both material processing and medical applications, the benefits extend beyond these applications. Specifically, a low pulse repetition rate during nonlinear amplification can substantially reduce the requisite amplifier pump power, thereby facilitating the generation of high-energy pulses. This reduction in power consumption not only enhances the system's energy efficiency but also permits the incorporation of cost-effective components, eliminating the necessity for active cooling. Moreover, an all-fiber scheme obviates the need for pulse-picking elements such as acousto-optical modulators, which are plagued by high insertion losses. Such modulators also necessitate supplementary control systems and RF drivers, thereby complicating the system and increasing its energy demands.

In this paper, we showcase an ultra-low repetition rate all-fiber GMN scheme adept at coherent pulse spectrum broadening, facilitating subsequent pulse compression. A numerical model of the fiber GMN amplifier has shown the ability to compress comparatively long pulses of picosecond duration into ultra-short ones with a repetition rate below 1 MHz. For the experimental demonstration of the developed model, an all-polarization-maintaining (PM) fiber laser has been designed. The generation of ultra-low repetition rate pulses is made possible through an all-fiber giant-chirp oscillator, as the first concept presented by Renninger et al [24]. For the experimental demonstration of the developed model, an all-PM fiber laser scheme has been designed. In order to generate mode-locked pulses with a low repetition rate, we constructed an all-polarization-maintaining figure-8 ultra-long fiber mode-locked seed laser. This fiber master oscillator was designed to produce highly chirped mode-locked picosecond pulses, providing adequate output power for direct GMN amplification in an all-PM fiber laser. We successfully

Optics EXPRESS

demonstrated GMN amplification of 32 dB of an ultra-long fiber mode-locked laser with PRR less than 1 MHz, achieving compressed pulses of 57 fs with GVD compensated, significantly down from the initial transform-limited pulse duration of 280 fs.

2. Theoretical model of the low PRR GMN amplifier

To simulate the nonlinear evolution of the pulse in the final stage of the system, we employ the generalized nonlinear Schrödinger equation (GNLSE) coupled with distributed rate equations to account for the interaction of the pulse with the doped core of the fiber.

The GNLSE for a scalar field in a doped medium reads:

$$\frac{dA(z,T)}{dz} = \hat{D}A + \hat{N}A + \frac{\hat{g}}{2}A. \tag{1}$$

Equation (1) includes dispersion operator $\hat{D}$, nonlinear operator $\hat{N}$, and operator associated with the interaction of the field with Yb ions, $\hat{g}$. The dispersion operator contains the coefficients β_k of the Taylor expansion series of propagation constant at a reference frequency:

$$\hat{D} = \sum_{k\geq 2} \frac{i^{k-1}\beta_k}{k!} \frac{\partial^k}{\partial T^k} \tag{2}$$

Here we omit the effect of passive losses as it is negligible at the considered wavelengths with a fiber length of several meters.

Accurate modeling of different repetition rate pulse amplifications in optical fibers can help optimize the amplification process for specific pulse energies [25]. The nonlinear operator includes both Kerr and Raman effects:

$$\hat{N}A = i\gamma\left(1 + \frac{1}{\omega_0}\frac{\partial}{\partial T}\right) \times \left[A(z,T)\int_{-\infty}^{+\infty} R(T')\,|A(z,T-T')|^2\,dT'\right]. \tag{3}$$

Here γ is the nonlinearity, ω_0 is the reference angular frequency, $R(t) = (1-f_R)\delta(t) + f_R h_R(t)$ is the nonlinear response function.

The operator of interaction with Yb ions $\hat{g}$ is spectral-dependent and therefore applied in the Fourier space. For some wavelengths, it provides gain, and for some other wavelengths, its effect manifests as loss, so we will also refer to it as a gain-loss operator. The amplitude gain-loss operator $\hat{g}/2$ is simply one-half of the intensity gain-loss operator $\hat{g}$ that we obtain from rate equations.

The effect of the amplitude gain-loss operator $\hat{g}/2$, when applied in the Fourier space, can be represented as:

$$\frac{\hat{g}}{2}A = \mathcal{F}^{-1}\left[\frac{g(z,\omega)}{2}\mathcal{F}(A)\right]. \tag{4}$$

Here the spectral-dependent intensity gain-loss $g(z,\omega)$ is calculated using quasi-stationary condition of the rate equations:

$$\begin{cases} \frac{dn_2}{dt} = 0 = \frac{[n_1\sigma_p^a - n_2\sigma_p^e]\Gamma_p}{\hbar\omega_p}P_p + f_{rep}\int_{-\infty}^{+\infty}\frac{[n_1\sigma^a(\omega) - n_2\sigma^e(\omega)]\rho(\omega)}{\hbar\omega}d\omega - \frac{\pi r_{core}^2}{\tau}n_2 \\ n_1 + n_2 = n_{Yb} \end{cases}. \tag{5}$$

Here $n_1 = n_1(z)$ and $n_2 = n_2(z)$ are the populations of the lower and upper states of Yb ions, σ_p^a, and σ_p^e are the absorption and emission cross sections at the pump wavelength, Γ_p is the pump-core overlap coefficient, $P_p = P_p(z)$ is the pump power, f_{rep} is the repetition rate of the pulse train, $\rho(\omega)$ is the energy spectral density of the pulse, r_{core} is the radius of the doped core

Optics EXPRESS

of the fiber, τ is the lifetime of the upper state of the Yb ion and n_{Yb} is the concentration of Yb ions. It should be noted that here, we assume that the overlap integral of the optical mode with the fiber core is equal to unity for every signal wavelength.

The energy spectral density $\rho(\omega) \propto |A(\omega)|^2$ satisfies:

$$\int_{-\infty}^{\infty} \rho(\omega) d\omega = \int_{-\infty}^{\infty} |A(T)|^2 \, dT \tag{6}$$

Given the populations n_1 and n_2, it is feasible to compute the pump absorption and the spectral-dependent gain for the signal:

$$\begin{cases} \frac{d\rho(z,\omega)}{dz} = g(z,\omega)\rho(z,\omega) = \left[\sigma^e(\omega)n_2(z) - \sigma^a(\omega)n_1(z)\right]\rho(z,\omega) \\ \frac{dP_p(z)}{dz} = \Gamma_p \left(\sigma_p^e n_2(z) - \sigma_p^a n_1(z)\right) P_p(z) \end{cases}. \tag{7}$$

Excluding n_1 from (5), (7) and considering (1–7), we obtain the following set of equations:

$$\begin{cases} \frac{dP_p}{dz} = -\left[\left(\sigma_p^e + \sigma_p^a\right) n_2(z) - \sigma_p^a n_{Yb}\right] P_p \\ \frac{dA(z,T)}{dz} = \sum_{k\geq 2} \frac{i^{k-1}\beta_k}{k!} \frac{\partial^k A}{\partial T^k} + i\gamma \left(1 + \frac{1}{\omega_0}\frac{\partial}{\partial T}\right) \times \left[A(z,T) \int_{-\infty}^{+\infty} R(T') \left|A(z,T-T')\right|^2 dT'\right] + \frac{\hat{\xi}}{2} A \\ g(z,\omega) = \left[\sigma^e(\omega) + \sigma^a(\omega)\right] n_2(z) - \sigma^a(\omega) n_{Yb} \\ n_2(z) = n_{Yb} \frac{\frac{\sigma_p^a \Gamma_p}{\hbar\omega_p} P_p(z) + f_{rep} \int_{-\infty}^{+\infty} \frac{\sigma^a(\omega)\rho(\omega)}{\hbar\omega} d\omega}{\frac{\left(\sigma_p^a + \sigma_p^e\right)\Gamma_p}{\hbar\omega_p} P_p(z) + f_{rep} \int_{-\infty}^{+\infty} \frac{\left[\sigma^a(\omega) + \sigma^e(\omega)\right]\rho(\omega)}{\hbar\omega} d\omega + \frac{\pi r_{core}^2}{\tau}} \end{cases}. \tag{8}$$

Table 1. Table of simulation parameters

Parameter name	Parameter value	Parameter name	Parameter value
Provided by the manufacturer		Calculated	
d_{core} (μm)	11.5	β_2 (ps^2/m)	1.8583×10^{-2}
$d_{\text{1st clad}}$ (μm)	125	β_3 (ps^3/m)	3.8775×10^{-5}
$\tilde{\alpha}_{\text{pump}}$ (dB/m)	6	β_4 (ps^4/m)	-4.7658×10^{-8}
NA	0.08	β_5 (ps^5/m)	1.6251×10^{-10}
The measured input pulse parameters		A_{eff} (μm^2)	8.3086×10^{1}
peak power (W)	42	γ (1/W/m)	2.4705×10^{-3}
pulse duration (ps)	1	$d\gamma/d\lambda$ (1/W/m/nm)	-9.5365×10^{-7}
energy (pJ)	30	n_{Yb} (1/nm^2/m)	2.6498×10^{8}

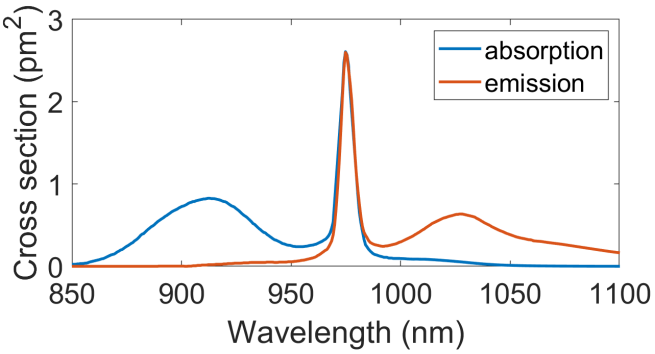

Fig. 1. Absorption and emission cross section Yb-doped PLMA DCF fiber [28].

Optics EXPRESS

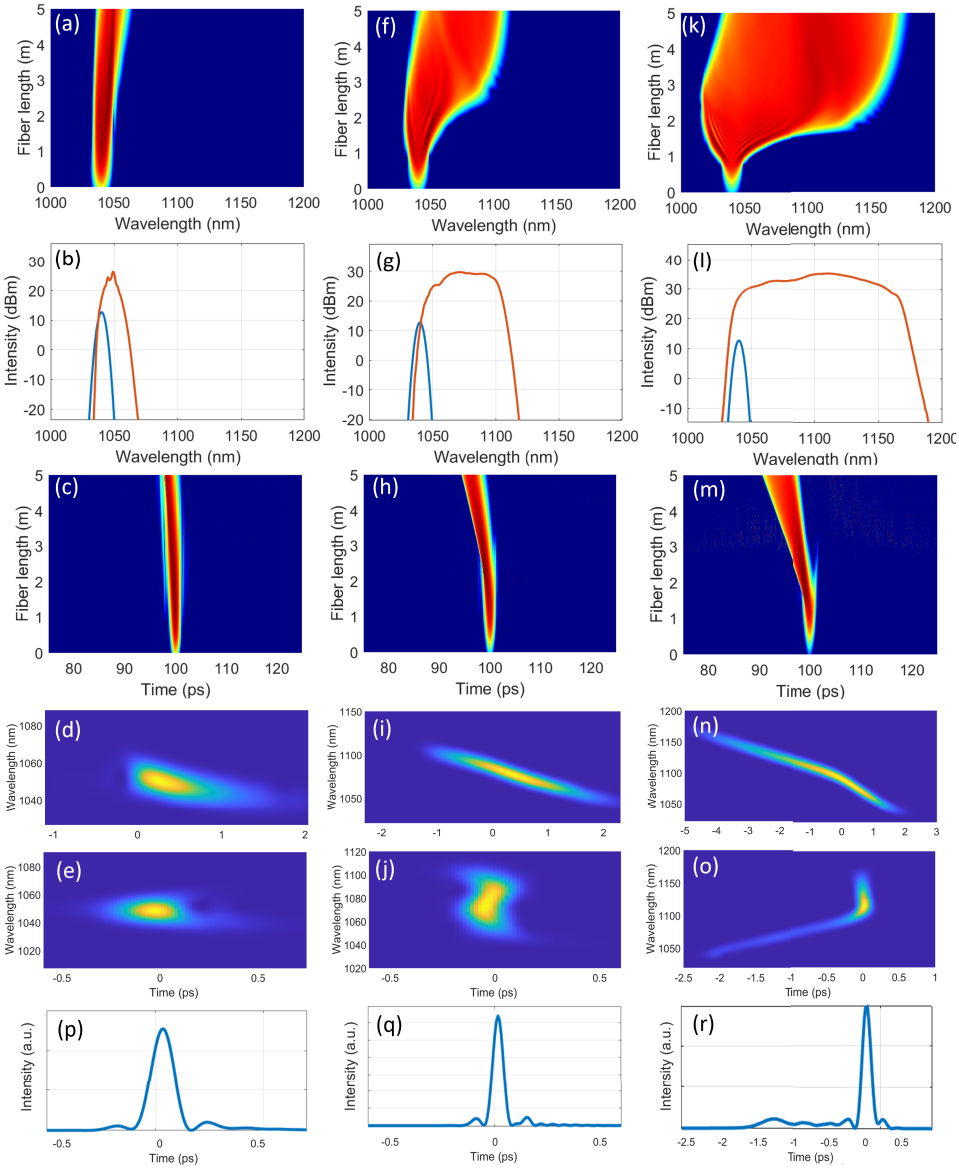

Fig. 2. Simulated pulse evolution with different PRRs in 5m Yb-doped PLMA DCF fiber. The spectral evolution, initial and output spectra, temporal pulse evolution and instantaneous frequency profiles of both uncompressed and compressed output pulses with pulse profiles for 100 MHz (a, b, c, d, e, p), 10 MHz (f, g, h, i, j, q), and 1 MHz (k, l, m, n, o, r) PRR seed laser, respectively.

which combined with initial conditions $P_p(z = 0) = P_0$ and $A(z = 0) = A_0$ closes the initial value problem statement and provides a theoretical framework for simulating GMN.

We used RK4IP method [26] for numerical integration. The simulation parameters are shown in Table 1. The fractional contribution of the delayed Raman response f_R was considered as 0.245 [27]. Nonlinear coefficient γ was derived from the fiber effective mode area, A_{eff} and the nonlinear index n_2 of silica, n_{Yb} was estimated using the fiber pump absorption $\bar{\alpha}_{\text{pump}}$ and the

Optics EXPRESS

absorption cross-section σ_a:

$$\bar{\alpha}_p = -\Gamma_p \sigma_p^a n_{Yb} \tag{9}$$

The fiber absorption and emission cross-sections provided by the supplier are depicted in Fig. 1 [28].

In order to utilize the full nonlinearity potential of 10/125 fiber with relatively long pulses, the PRR could be reduced. The modeling results of the impact of GMN amplification on picosecond pulses with varying repetition rates are illustrated in Fig. 2. To make the effect more evident, the evolution of a 1-picosecond pulse was examined for different PRRs, ranging from 100 MHz to 1 MHz. By adjusting the average power at the input of the GMN amplifier, the peak power, pulse energy, and duration were maintained constant for pulses with different PRRs. It was found that at lower PRR with a pulse duration of approximately 1 ps, GMN spectral broadening is observed, displaying a wider coherent structure accompanied by a small Raman shoulder component. Figure 2 demonstrates simulation results, which confirm the possibility of getting more than 100 nm wideband for 1 picosecond pulse at a 1 MHz PRR. The long-wavelength edge of generated coherent spectra reaches 1150 nm. The spectra for the lowest PRR seed source are broader than those for the high-repetition-rate source and therefore support shorter pulse durations at the same pump power. Further spectrum broadening is limited by the nonlinearity and the rise of the non-coherent Raman radiation, which begins to prevail in the output signal. The results match the previously published outcomes of developing a GMN amplifier on the PLMA 10/125 fiber for the pulses with a repetition rate of tens of 10 MHz.

3. Experimental setup

To substantiate our findings, we developed an experimental setup based on the numerical modeling results. Intending to preserve the all-PM passive fiber mode-locked laser concept, we designed an ultra-long fiber laser cavity to generate low-repetition-rate pulses, thereby eliminating the need for acousto-optical pulse pickers.

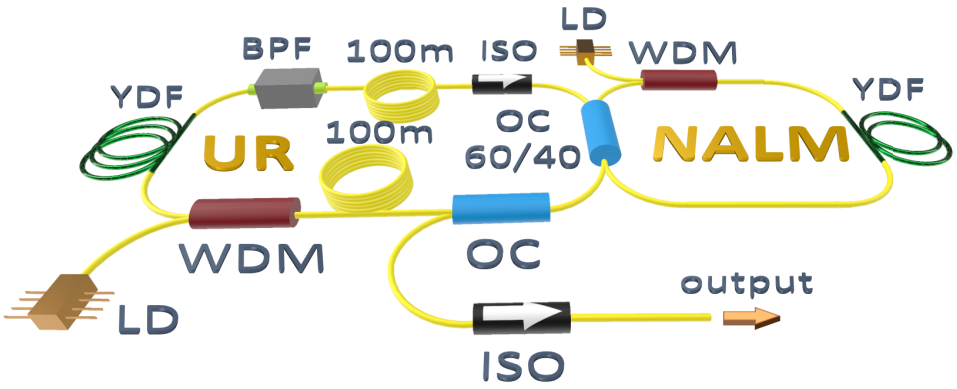

Fig. 3. Experimental setup of low PRR mode-locked all-PM fiber Yb laser, LD - laser diode; BPF - band pass filter, WDM - wavelength division multiplexer, YDF - ytterbium-doped fiber; 100 m of passive PM fiber, ISO - fiber isolator, OC - optical coupler.

The setup of a long all-polarisation-maintaining (PM) fiber seed laser with a repetition rate of 950 kHz and generated pulse duration of 40 ps at 1040 nm was assembled. The laser cavity layout is shown in Fig. 3. It comprised two loops, including a main uni-directional (UR) section and a nonlinear amplifying loop mirror (NALM). The main loop comprised up to 200 m of fiber in two spools, a 3 m low Yb-doped fiber (YDF), a polarisation-dependent optical isolator (ISO), a wavelength division multiplexer (WDM), a 50:50 output coupler (OC), and a narrow 2 nm

Optics EXPRESS

bandpass filter (BPF) centered at 1040 nm. The NALM loop, which was bidirectional, functioned to mode-lock the laser. It incorporated a length of the passive fiber and a short segment of highly doped Yb fiber. This Yb fiber was pumped by a laser diode (LD) via another wavelength division multiplexer (WDM). The loop was connected to the main loop via a 60:40 central coupler (OC 60/40). The two separately pumped gain sections allowed for an additional degree of freedom in mode locking, permitting fine-tuning of the output pulse characteristics. The ultra-long UR loop structure comprises two long spools (100m length each), enabling the creation of an all-normal dispersion Yb mode-locked fiber laser capable of generating broadband pulses with ultralow repetition rates. Stable pulse trains with repetition rates as low as 950 kHz have been achieved by carefully positioning fiber sections in the all-PM fiber cavity [29].

In the double-spool laser configuration, a noise-like pulse regime was initially generated, which then transitioned to a mode-locked regime upon the reduction of pump power. In a single pulse mode-locking operation, the laser produced a repetitive pulse train with a clean radio frequency (RF) spectrum, as shown in Fig. 4. The measured signal-to-noise ratio (SNR) was 62 dBm, indicating stable single-pulse mode-locking. The generated spectrum at 1040 nm had a full width at half-maximum (FWHM) of approximately 7 nm and steep edges, characteristic of ANDi lasers. The output power was measured as 1.4 mW and highly chirped pulses had a duration of 40 ps (FWHM). The spectrum of the input pulse that is fed into the GMN amplifier is shown in Fig. 4(b).

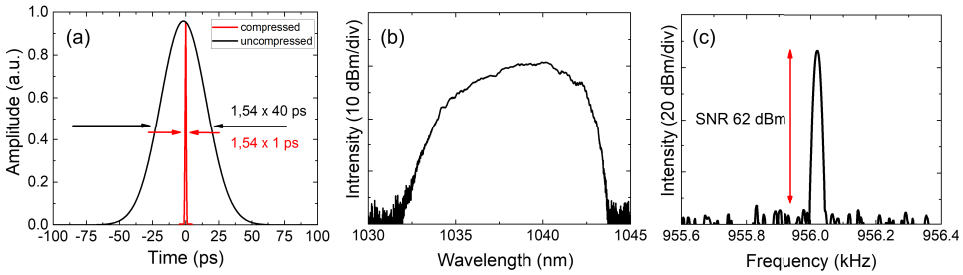

Fig. 4. Measured (a) seed pulse autocorrelation traces before (black) and after (red) compression stage, (b) optical and (c) RF spectra of developed low PRR mode-locked all-PM fiber Yb laser.

Utilizing the pulse compression stage at the seed output, the pulse duration was reduced to 1 ps, although it retained a slightly positive chirp. Although the transform-limited pulse duration for the generated 7 nm bandwidth spectrum could potentially reach a duration shorter than 300 fs, a 1 picosecond pulse duration was selected to minimize nonlinear effects within the PM-980 fiber prior to the GMN amplifier stage. Notably, employing passive fiber Bragg Grating (FBG) compressors for picosecond pulse duration compression contributes to a more compact system, as opposed to the Treacy pulse compression scheme, which is predicated on the utilization of a pair of diffraction gratings [30]. To implement the fiber Bragg grating (FBG) compressor and enable additional control, a fiber variable optical attenuator (VOA) was placed at the output of the seed laser. The scheme of the GMN amplifier is shown in Fig. 5. The system consists of a PM pump combiner, a high-power laser diode, and 5 m of PM double-clad fiber (DCF) from Coherent's PLMA-YDF-10/125-VIII series. The measured absorption and calculated emission cross-sections of the PLMA-YDF-10/125-VIII are also presented in Fig. 1. The end of active DCF fiber was angle cleaved to avoid back reflection. An aspherical lens and a long-pass filter were installed at the output of the active fiber to block any residual 980 nm pump.

Figure 5 depicts the final scheme of the laser with a GMN amplifier. The low power threshold of around 30 μW gives a chance to avoid any pre-amplification stages.

Optics EXPRESS

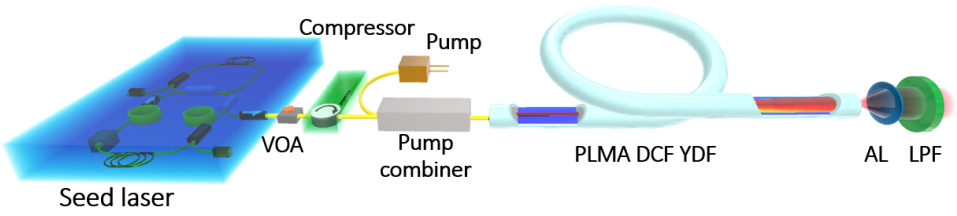

Fig. 5. Schematic of the GMN amplification system.VOA - variable optical attenuator; PLMA DCF YDF - polarization-maintaining large mode area double clad ytterbium-doped fiber; AL - aspherical lens; LPF - longpass filter.

4. Results and discussion

Figure 6 depicts the spectral broadening at different 980 nm pump power levels for a pulse with a PRR of 956 kHz, a duration of 1 ps, and an average power of around 30 µW. The reduced average power, owing to the low PRR signal, extended the nonlinear length and curtailed the impact of nonlinear effects within the all-fiber setup prior to the GMN amplifier. The figure presents the evolution of the amplified spectrum as a function of the pump power for an ultra-low PRR seed source after passing through an amplifier. The continuous wave 980 nm pump power increased from 622 mW to 1202 mW. As the pump power increases, the spectrum broadens significantly. The measured bandwidth extends beyond 1100 nm, exceeding the bandwidth of the Yb-doped double-clad fiber (DCF). When the output pulse energy surpasses 60 nJ, Raman scattering becomes observable. As the pump power exceeds 1000 mW, a low-intensity spectral shoulder distinct from the main pulse becomes evident. At the highest pump power levels, the Raman contribution becomes more significant. Following the GMN amplifier, the pulse duration expanded from 1 ps to 6.03 ps. We observe a non-negligible Raman contribution in the experimental spectra, which hampers the pulse compression ability.

The experimental results align with the simulation outcomes, suggesting that Raman contributions primarily shape secondary pulse structures separate from the main temporal pulse. The coherence of the Raman component in relation to the main pulse is weak. This can be clearly identified using a standard optical spectrum analyzer (OSA) and frequency-resolved optical gating (FROG). Figures 7(a) and 7(b) illustrate the FROG measured and retrieved traces of the GMN amplified single broadband pulse at a pump power of 982 mW.

At the highest pump power (1202 mW), the Raman contribution was more than 41% (Fig. 6). For further investigation of pulse compression ability, we halted the pump power at 982 mW as a suitable balance between high output power and mitigation of secondary Raman pulses. In this case, the Raman contribution was around 2%. Furthermore, we recorded a 17 dB difference in intensity between the main pulse and the Raman shoulder of the amplified pulse spectra. In this regime, the spectral bandwidth was measured as 91 nm, corresponding to a transform-limited pulse duration of 17 fs. The initial average power of the pulse was attenuated to 30 µW and subsequently amplified to 52 mW. This corresponds to an amplification of 32 dB. The transparency of the long pass filter (LPF) for the 980 nm pump was considered. After blocking the unsaturated 980 nm pump with the LPF, the final pulse energy was estimated to be 52.6 nJ

By using a grating compressor, we managed to dechirp the amplified pulses. The pulse duration post-compression was significantly shorter than the initial transform-limited duration of 280 fs. This indicates that the generated bandwidth is coherent and not a result of shot-noise-seeded Raman scattering, suggesting that the pulse evolves to a nonlinear attractor and that the Yb-based GMN amplifier is operating correctly.

Figure 8(a) depicts the initial pulse spectra, centered at 1040 nm with a bandwidth of around 7 nm at FWHM, and the final spectra after the LMA GMN amplifier stage, which has a bandwidth

Optics EXPRESS

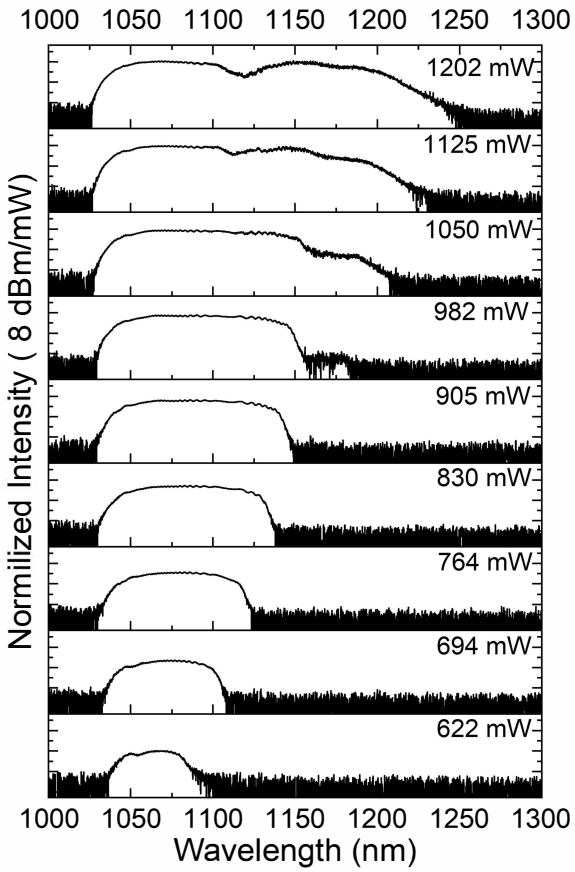

Fig. 6. Spectral measurements for varying pump power of the GMN amplifier. PRR of the seed laser is 956 kHz.

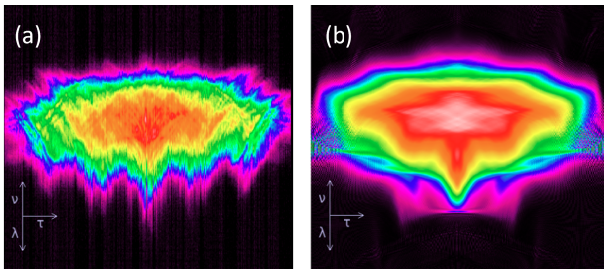

Fig. 7. FROG trace of GMN amplified pulses: (a) measured and (b) retrieved trace at a pump power of 982 mW where ν-frequency, λ-wavelength, τ-time.

Optics EXPRESS

of 91 nm and a central wavelength of around 1100 nm. For comparison, we have included the spectrum resulting from numerical simulation, which aligns well with the experimental results. Figure 8(b) shows the measured autocorrelation traces of the initial 1 ps pulse at the input of the GMN amplifier and the dechirped pulse duration of 57 fs, achieved using the Treacy compression scheme. We note that 83% of the energy is in the main pulse, with only 17% distributed in the uncompressed pedestal.

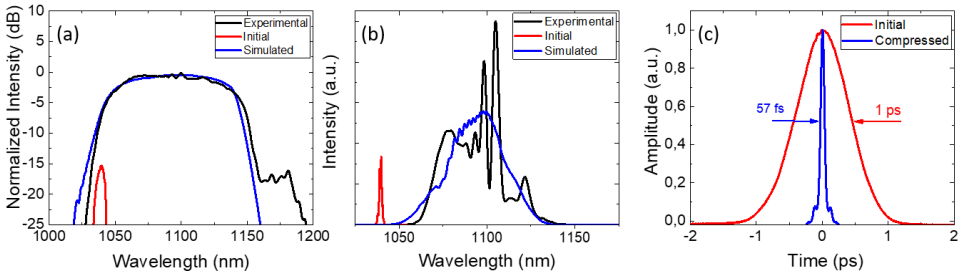

Fig. 8. Characterization of the amplified 1 ps pulses for the 956 kHz laser source at 982 mW pump power: in the logarithmic (a) and linear scales (b) comparison of the simulated (blue), measured (black) spectra at the output of the amplifier with the corresponding seed pulse spectrum (red); Comparison of the autocorrelation traces of the initial pulse (red) and the amplified GVD-compensated pulse (blue) (c).

The obtained pulse duration of 57 fs, although longer than the Fourier-transform limit of 17 fs, is mainly attributed to the non-compensated higher-order dispersion and challenges in aligning the diffraction gratings. Misalignments can induce phase shifts in diffracted light, potentially deviating from the transform-limited pulse duration. Nevertheless, this duration is still notably shorter than the initial 280 fs. The difficulty in fully compensating for higher-order dispersion complicates the application of ultra-long all-fiber oscillators as seed lasers, especially when targeting repetition rates lower than our current one.

We successfully demonstrated an all-PM fiber scheme with GMN amplification exceeding 32 dB for an ultra-long mode-locked all-PM fiber laser. The resulting pulses exhibited a duration of approximately 57 fs, indicating a substantial compression from the initial transform-limited duration of 280 fs. To our knowledge, this is the first published example of this type of an all-PM fiber laser scheme and a study of the GMN amplification regime for low pulse repetition rate ultra-long mode-locked laser.

5. Conclusion

In this study, we have both theoretically and experimentally investigated the GMN amplification of a mode-locked seed laser with a PRR of less than 1 MHz. Our simulation results closely align with our experimental data, demonstrating the ability of GMN amplification of low-energy pulses at a low repetition rate. The experiment involved feeding a 1 ps seed pulse to the amplifier, with 0.03-nJ pulses generated by a self-built, all-PM, ultra-long 8-figure Yb mode-locked fiber laser. In the first demonstration of the benefits of GMN amplifiers for low PRR lasers, we attained a pulse with a bandwidth exceeding 91 nm and a signal gain of 32 dB within an all-PM fiber laser scheme.

Funding. H2020 Future and Emerging Technologies (863214); Engineering and Physical Sciences Research Council (EP/W002868/1).

Acknowledgments. DS and EM acknowledge the support of the EPSRC project EP/W002868/1. DS, AK, and ER acknowledge the support of the European Union's Horizon 2020 Research and Innovation Programme under Grant 863214.

Optics EXPRESS

Disclosures. The authors declare no conflicts of interest.

Data availability. The datasets generated and analyzed during the current study are available from the corresponding author upon reasonable request.

References

1. M. E. Fermann and I. Hartl, "Ultrafast fiber laser technology," IEEE J. Sel. Top. Quantum Electron. **15**(1), 191–206 (2009).
2. W. Zhao, X. Hu, and Y. Wang, "Femtosecond-pulse fiber based amplification techniques and their applications," IEEE J. Sel. Top. Quantum Electron. **20**(5), 512–524 (2014).
3. D. Strickland and G. Mourou, "Compression of amplified chirped optical pulses," Opt. Commun. **55**(6), 447–449 (1985).
4. S. Zhou, L. Kuznetsova, A. Chong, *et al.*, "Compensation of nonlinear phase shifts with third-order dispersion in short-pulse fiber amplifiers," Opt. Express **13**(13), 4869–4877 (2005).
5. Y. Zaouter, D. N. Papadopoulos, M. Hanna, *et al.*, "Stretcher-free high energy nonlinear amplification of femtosecond pulses in rod-type fibers," Opt. Lett. **33**(2), 107–109 (2008).
6. H.-W. Chen, J. Lim, S.-W. Huang, *et al.*, "Optimization of femtosecond yb-doped fiber amplifiers for high-quality pulse compression," Opt. Express **20**(27), 28672–28682 (2012).
7. D. A. Korobko, O. G. Okhotnikov, D. A. Stoliarov, *et al.*, "Highly nonlinear dispersion increasing fiber for femtosecond pulse generation," J. Lightwave Technol. **33**(17), 3643–3648 (2015).
8. D. A. Korobko, O. G. Okhotnikov, D. A. Stoliarov, *et al.*, "Broadband infrared continuum generation in dispersion shifted tapered fiber," J. Opt. Soc. Am. B **32**(4), 692–700 (2015).
9. I. Zolotovskii, D. A. Korobko, O. G. Okhotnikov, *et al.*, "Generation of a broad ir spectrum and-soliton compression in a longitudinally inhomogeneous dispersion-shifted fibre," Quantum Electron. **45**(9), 844–852 (2015).
10. W. Fu, Y. Tang, T. S. McComb, *et al.*, "Limits of femtosecond fiber amplification by parabolic pre-shaping," J. Opt. Soc. Am. B **34**(3), A37–A42 (2017).
11. M. E. Fermann, V. Kruglov, B. Thomsen, *et al.*, "Self-similar propagation and amplification of parabolic pulses in optical fibers," Phys. Rev. Lett. **84**(26), 6010–6013 (2000).
12. V. Kruglov, A. Peacock, J. Dudley, *et al.*, "Self-similar propagation of high-power parabolic pulses in optical fiber amplifiers," Opt. Lett. **25**(24), 1753–1755 (2000).
13. P. Sidorenko, W. Fu, and F. Wise, "Nonlinear ultrafast fiber amplifiers beyond the gain-narrowing limit," Optica **6**(10), 1328–1333 (2019).
14. P. Mamyshev, "All-optical data regeneration based on self-phase modulation effect," in *24th European Conference on Optical Communication. ECOC'98 (IEEE Cat. No. 98TH8398)*, vol. 1 (IEEE, 1998), pp. 475–476.
15. V. Boulanger, M. Olivier, F. Trépanier, *et al.*, "Multi-megawatt pulses at 50 mhz from a single-pump mamyshev oscillator gain-managed amplifier laser," Opt. Lett. **48**(10), 2700–2703 (2023).
16. P. Sidorenko and F. Wise, "Generation of 1 μj and 40 fs pulses from a large mode area gain-managed nonlinear amplifier," Opt. Lett. **45**(14), 4084–4087 (2020).
17. D. Tomaszewska-Rolla, R. Lindberg, V. Pasiskevicius, *et al.*, "A comparative study of an yb-doped fiber gain-managed nonlinear amplifier seeded by femtosecond fiber lasers," Sci. Rep. **12**(1), 404 (2022).
18. H. Pask, R. J. Carman, D. C. Hanna, *et al.*, "Ytterbium-doped silica fiber lasers: versatile sources for the 1-1.2/spl mu/m region," IEEE J. Sel. Top. Quantum Electron. **1**(1), 2–13 (1995).
19. S. M. Eaton, H. Zhang, P. R. Herman, *et al.*, "Heat accumulation effects in femtosecond laser-written waveguides with variable repetition rate," Opt. Express **13**(12), 4708–4716 (2005).
20. C. L. Evans and X. S. Xie, "Coherent anti-stokes raman scattering microscopy: chemical imaging for biology and medicine," Annu. Rev. Anal. Chem. **1**(1), 883–909 (2008).
21. C. J. Engelbrecht, R. S. Johnston, E. J. Seibel, *et al.*, "Ultra-compact fiber-optic two-photon microscope for functional fluorescence imaging in vivo," Opt. Express **16**(8), 5556–5564 (2008).
22. N. H. Rizvi, "Femtosecond laser micromachining: Current status and applications," Riken review pp. 107–112 (2003).
23. C. Lefort, "A review of biomedical multiphoton microscopy and its laser sources," J. Phys. D: Appl. Phys. **50**(42), 423001 (2017).
24. W. H. Renninger, A. Chong, and F. W. Wise, "Giant-chirp oscillators for short-pulse fiber amplifiers," Opt. Lett. **33**(24), 3025–3027 (2008).
25. R. Lindberg, P. Zeil, M. Malmström, *et al.*, "Accurate modeling of high-repetition rate ultrashort pulse amplification in optical fibers," Sci. Rep. **6**(1), 34742 (2016).
26. J. M. Dudley and J. R. Taylor, *Supercontinuum generation in optical fibers* (Cambridge University Press, 2010).
27. Q. Lin and G. P. Agrawal, "Raman response function for silica fibers," Opt. Lett. **31**(21), 3086–3088 (2006).
28. Coherent UK Ltd. Private correspondence.
29. P. Bowen, M. Erkintalo, R. Provo, *et al.*, "Mode-locked yb-doped fiber laser emitting broadband pulses at ultralow repetition rates," Opt. Lett. **41**(22), 5270–5273 (2016).
30. E. Treacy, "Optical pulse compression with diffraction gratings," IEEE J. Quantum Electron. **5**(9), 454–458 (1969).